www.rericjournal.ait.ac.th

Fermented Cassava-rhizome Residue as a Biomass Pellet Binding Additive Influenced by Multi-bacterial Biofilm

Weeranut Intagun*, [1], Nitipong Soponpongpipat*, and Wirojne Kanoksilapatham*

ARTICLE INFO

Article history:
Received 16 June 2023
Received in revised form
24 August 2023
Accepted 12 October 2023

Keywords:
Cassava rhizome
Biofilm
Biofuels biomass pellets
Fermented cassava rhizome
Leucaena wood

ABSTRACT

The use of fossil fuels can be reduced by using biomass fuels. As one of the world's largest producers of cassava, starch-rich cassava-rhizome waste is readily available for direct and indirect energy sources. Using a simple fermentation method, the binding properties of fermented cassava-rhizome were considerably enhanced. The investigation was conducted by comparing the bulk density, durability index, production yield, and higher heating value of pellet made from Leucaena-wood residue, Leucaena-wood residue mixed with fermented and non-fermented cassava rhizome. The biofilm produced by the growing microorganisms on the fermentation particles played an important role in improving the binder's quality. The biofilm provided stronger adhesive force than starch contained in non-fermented cassava rhizome. It was demonstrated by the increase in bulk density and durability when fermented cassava rhizome was mixed into pellets. In the early stages of incubation, the conversion of starch to the microbial biofilm did not significantly affect the higher heating value of the cassava rhizome. However, prolonged fermentation caused a decrease in the higher heating value. Day 3 of incubation was the optimal fermentation time. After day 3, rotting biomass fibers increased, which decreased the durability of pellets made from the additives.

1. INTRODUCTION

Biomass pellets and other forms of bioenergy are growing in popularity and demand as a way to reduce the use of fossil fuels [1]–[3]. As one of the world's major cassava plant-growing countries, with a production of ca. 29.3 million tons/year, a considerable volume of cassava-rhizome residue is available for direct and indirect biofuel resources [4], [5]. Pelletizing small fragments of biomass raw materials into cylindrical pellet forms, with or without a binding agent, can alleviate the problems caused by bulky structures and labour-intensive processing [6], [7]. High-quality biomass pellets aid in the prevention of damage during storage and transportation. The quality of biomass pellets can be assessed through their resistance to mechanical collision, compression force, and water breakage [8]–[14].

The three major plant biomass polymers (cellulose, hemicellulose, and lignin) contain a wide range of functional groups that can form electro-attractive forces, cohesively link inter-particulates together, and strengthen biomass pellet matrices. Cellulose, an insoluble, long-linear polysaccharide chain of glucose, can interact with hemicellulose and lignin primarily through the outer hydroxyl groups (OH) on its glucose chains [15]. Hemicellulose, a short-branched polysaccharide of pentose and hexose sugars as well as those sugars' acidified versions, can establish ionic and covalent interactions with divalent cations as well as lignin by utilizing the carboxylic groups (COO^-) on the acidic sugars [15]-[17]. Lignin contains hydroxyl, methoxyl ($O\text{-}CH_3$), aromatic rings, and phenyl-propane units [15], [18]-[19]. Methoxyl groups attached to aromatic rings can delocalize and increase electron density within the conjugated ring structure. Starch, a soluble amorphous polysaccharide of helical and branch chains of glucose, can gelatinize with heat and moisture and then change to a viscous fluid that strengthens the pellet matrix during the pelletizing process, unlike cellulose [15], [17], [19]–[20].

Microorganisms excrete extracellular polymeric substances (EPS) to help stick to solid surfaces, maximize growth, and provide growth compartments and conditions, also known as "microbial biofilms". Biofilms are single or multispecies microbial communities encased in a slimy matrix formed on solid surfaces. They are found in a wide range of natural and artificial habitats and are composed of a mixture of extracellular polymeric substances, including mainly polysaccharides, some proteins, polynucleotides, and lipids [21]–[26]. Biofilm structures and chemical compositions have been well known and characterized. The chemical structures of biofilm polysaccharides from gram-negative symbiotic rhizobia were found to be

*Department of Mechanical Engineering, Faculty of Engineering and Industrial Technology, Silpakorn University, Nakhon Pathom 73000, Thailand.

[1]Corresponding author:
Tel: + 66850332770.
Email: weeranut_n@hotmail.com

made up of a variety of sugars and acidic sugars [22]. Biofilm polysaccharides from gram-positive staphylococci were classified based on polarity into two groups: the major group (ca. >80%) has more positively charged functional groups like N-acetylhexosamines, and the minor group (ca. 20%) has more negatively charged residues such as phosphate groups, ester-linked succinate moieties, and fewer deacetylated residues [23], [27]. Biofilm matrices of two species of a yeast-like fungi play a role as sticky materials and contain varying amounts of amino sugars, carbohydrates, glucose, uronic acid, protein, and phosphorus [25]. Alginate, a bacterial biofilm polysaccharide, can form strong ionic interactions with divalent cations such as Ca^{2+}, Mg^{2+}, and Mn^{2+} before becoming hydrated and transforming into a sticky gel [24], [28]-[32].

Certain biomass pellets may have a weak matrix, making them susceptible to mechanical fracture and requiring a binding additive [29], [33]-[35]. The primary goal of this research is to improve the binding quality of cassava rhizome residue, a starch-containing agricultural waste that can be used as an inexpensive biomass pellet additive. A simple and energy-efficient microbiological method was applied because heat sterilization is not required to prepare cassava rhizome biomass raw materials. The physical change of the cassava rhizome during the fermentation process is investigated by means of scanning electron microscopy (SEM). Pellet properties, including bulk density, durability index, and higher heating value, were employed to study the quality of cylindrical pellet products. The quality of pellets made with the addition of non-fermented and fermented cassava rhizomes was compared. Finally, variation in the binding property of fermented cassava rhizomes at different incubation periods was studied.

2. MATERIALS AND METHODS

2.1 Biomasses

After goats were fed the leaves and bark of *Leucaena leucosephala* (a rapidly growing leguminous tree with the potential to be utilized for biomass fuel or charcoal production), the wood residues were recovered from the Cha-am District, Phetchaburi Province, Thailand. Cassava-rhizome (Cr) residues were obtained from Damnoen Saduak District, Ratchaburi Province, Thailand. In this study, the Leucaena-wood residue (L) was employed to compare the adhesiveness of Cr and several fermented Cr additions. According to previous work [36], cassava rhizome and Leucaena-wood particles were prepared as follows, biomass residues were cleaned and sundried. The cleaned biomasses were then chopped, pounded, crushed, and sieved to obtain small bits (ca. 0.5 mm in size). Moisture contents were assayed at 105 ºC for 24 h using a hot air oven.

2.2 Preparation of Fermented Cr (FCR) Additives and Microbial Growth

2.2.1 Microorganisms

Because significant amounts of soil microorganisms are always contaminated with Cr residues (even after cleaning). In this study, microorganisms from Cr raw materials were used as a natural inoculum to prepare fermented Cr particles without isolating a pure culture.

2.2.2 Fermentation

To create biofilm-based Cr, ground, non-sterile Cr particles were used directly (no heat sterilization) as the only substrate to cultivate soil microorganisms using a simple microbiological technique. To summarize, Cr particles (1.8 kg) were thoroughly moistened with water (0.6 kg) and incubated at room temperature for 1, 3, 5, 7, and 12 days. Aeration was provided during fermentation by turning over the fermenting materials twice daily. Three replicates were carried out for each fermentation duration. Microbial growths were examined, as well as biofilms. The fermented Cr (FCR), which contains D1FCr, D3FCr, D5FCr, D7FCr, and D12FCr, was compared to the non-fermented one (D0FCr or NFCR) as a binding additive.

2.2.3 Enumeration of common soil bacteria and detection of dominant population

Triplicate fermentation trials were performed. To detect bacterial growth, samples were taken daily, and a serial dilution spread plate method and nutrient agar plates (three replicates for each sample) were employed to count bacterial numbers. The results revealed a reproducible bacterial growth profile. Bacterial cell density was increased. To detect bacterial morphology and staining characteristics, Gram's staining technique and a light microscope were used. Figure 1 depicts various shapes and densities of gram-positive and gram-negative bacteria found to be dominant in the cultures, indicating the presence of multiple types of bacteria. No yeast was detected at the beginning of fermentation (days 1 and 2). A few yeasts were also found from day 3 onward.

Despite the fact that cassava contains cyanogenic glycosides, which are toxic to cellular respiration when broken down to HCN compounds, many traditional fermented cassava-food products have been made [37], [38]. This study's reproducible growth confirmed that Cr residue does not inhibit microbial growth; however, the initial growth phase may be delayed.

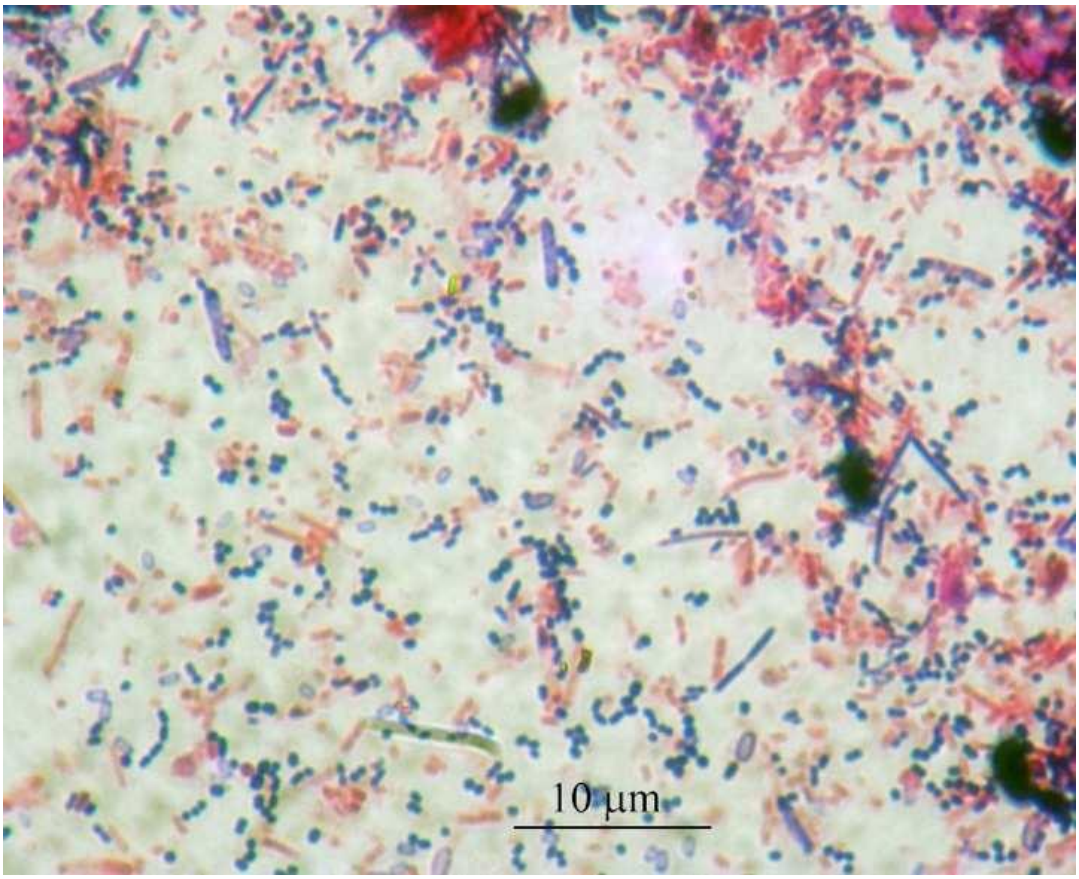

Fig. 1. A gram-staining microscopic image shows reproducible results of a dense number and various shapes of bacteria, including gram-positive endospore-forming rods, free endospores, gram-positive spherical-shaped bacteria, and gram-negative rod-shaped bacteria. A few yeast-like fungi stained with gram-positive color were also detected on day-3 samples (the image was taken from a representative sample collected on day 3 of fermentation).

2.3 Scanning Electron Microscopy (SEM)

In order to demonstrate the presence of starch and biofilms, a high-resolution analytical SEM (TESCAN MIRA3) was used to examine the surface textures of Cr biomass samples. The samples include non-fermented Cr (D0FCr) and fermented Cr (D3FCr, and D12FCr) particles. Carbon adhesive tape was used to mount the specimen on a metal stub. The stub was gold sputter coated and stored in a desiccator.

2.4 Pelletizing Experiments

A rotary flat-die pellet mill (KL200B Model, China), operating at a speed of 278 rpm, was used to pelletize biomass into a cylindrical pellet shape (6.5±0.1 mm in diameter). The starting temperature was raised to roughly 75ºC by pressing rice bran through the die channels. A total dry biomass of 6 kg was set aside for each procedure. At the end of the process, a die temperature of >90ºC was detected. Before being tested for bulk density, mechanical durability, and other parameters, all of the cylindrical pellet products obtained were kept at room temperature for one day.

2.4.1 Preparation of Leucaena pellet (L pellet)

Leucaena-wood (L-wood) particles (6 kg) were humidified with water (1.2 kg). The ingredients were kept at room temperature for 2 hours before being pelletized into hot die press channels. Three pelletizing trials of *Leucaena pellet (L-pellet)* were repeated.

2.4.2 Preparation of Leucaena and non-fermented Cr (L-NFCR) composite pellet

In order to produce L-NFCR pellet, 4.2 kg of L-wood particles were mixed with 1.2 kg of water and 1.8 kg of non-fermented Cr (NFCR or D0FCr) particles. The additive was estimated to be around 30% of the total biomass weight. The ingredients were kept at room temperature for 2 hours before being pelletized into hot die press channels. The procedure was repeated three times.

2.4.3 Preparation of Leucaena and fermented Cr (L-FCR) composite pellet

To maintain a constant total biomass of 6 kg and a 30% additive (relative to the total biomass), L-FCR pellets were prepared by mixing 4.2 kg of L-wood particles with 0.6 kg of water and 2.4 kg of fermented Cr (FCR) particles. The latest ingredient is composed of 1.8 kg of Cr and 0.6 kg of water, as mentioned in Section 2.2.2 *Fermentation*. The ingredients were kept at room temperature for 2 hours before being pelletized into hot die-press channels. For each fermentation condition, the procedure was repeated three times.

2.5 Determination of Standard Bulk Density, Durability Index and Production Yield

2.5.1 Bulk density

The bulk density index (kg/m^3) of the cylindrical pellet

products was evaluated using the method described in ASTM E 873-82 in a standard chamber (305 x 305 x 305 mm^3) [39].

2.5.2 Durability index

The pellet products' resistance to mechanical break was determined following the PFI standard procedure for Durability Testing. Biomass pellet (0.5 kg) in a standard chamber (305 x 140 x 305 mm^3) was tumbled at 50 rpm for 10 min. After the tumbling, the content was sieved through a 1⁄8-inch sieve. The retained pellets on the sieve were weighted using an analytical balance. The durability index was calculated as a percentage of the initial weight.

2.5.3 Pellet production yield

The pellet production yield was defined as the ratio of the mass of pellets obtained from the pellet mill to the mass of raw biomass fed into the pellet mill.

2.6 Higher Heating Value (HHV)

The procedure described in ASTM E 711-87 [40] was used to determine higher heating values (HHVs). Before the analysis, the moisture in the samples was essentially removed overnight in an oven at 105°C. Five replicates for each pellet sample were conducted. Error bars were calculated with a confidence level of 90%.

3. RESULTS AND DISCUSSION

3.1 SEM Studies

3.1.1 Starch granule in non-fermented Cr

SEM images of the ground NFCR (D0FCr) shows uneven sizes and shapes (Figure. 2a), a layer rich in starch granules (Figure 2c), and a few carry-over granules on wood fragments (Figure 2b and Figure 2d).

3.1.2 Biofilm on fermented Cr

Microbial biofilms ubiquitously found on damp solid surfaces have slimy characteristic [21]-[26]. Figure 3 shows multi-bacterial biofilms developed on the D3FCr particles. Starch granules vanished when compared to D0FCr (Figure 2), implying that they were used as nutrients for growth and biofilm conversion. Figures 3a and 3b depict filamentous bacteria. Figure 3d shows coccus-shaped bacteria. In Figure 1, various types of bacteria detected as dominants on the day 3 fermented particles suggest multi-bacterial species. On day 3, a few yeast-like fungi can also be found (Figure 1). As a result, mixed types of biofilms were produced, which should be referred to as microbial biofilms. The finding shows similar slimy features to the previous report on yeast biofilm forming on the PVC catheter disks [25].

3.1.3 Decaying biomass fiber

Biofilm was also detected on the D12FCr sample (Figure 4). As a result of microbial hydrolytic enzymes, a massive increase in rotting biomass fibers was detected after long periods of fermentation (Figure 4a). The results suggest that fiber strength has decreased.

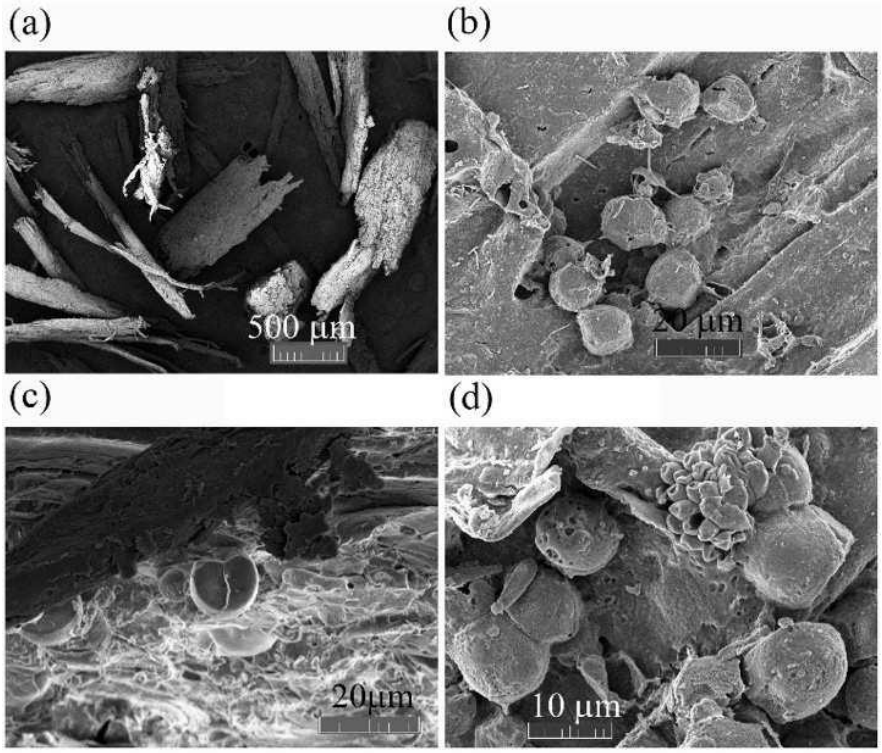

Fig. 2. SEM image of the ground D0FCr particles. (a) Variation in particle sizes and shapes of the Cr residue. (b) Starch granules on the surface of a piece of wood particle. (c) Starch rich-hyaline sacs. (d) Dome shaped starch granules (the scales are as indicated).

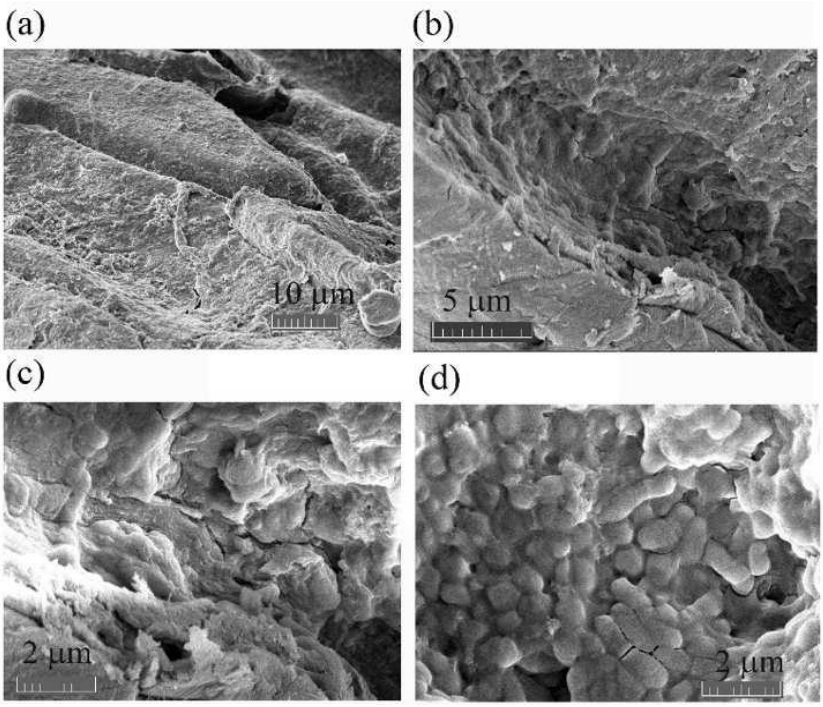

Fig. 3. SEM images of the D3FCr particles. (a-b) A biofilm on fermented particles (c-d) Filamentous and short rod-shaped bacteria in a thick layer of slimy biofilm (the scales are as indicated).

3.2 Fermented and Non-fermented Cr as a Natural Binding Additive

The addition of a FCR or NFCR to L-pellets increased their bulk density (Figure 5). L-pellet had the lowest bulk density of 618.4 ± 2.0 kg/m^3. Adding NFCR to L-pellet (D0FCr-L) increased the bulk density by 3.9% (642.6 ±2.9 kg/m^3). The highest bulk density was 668.9 ± 1.54 kg/m^3 when D3FCr was added. When durability was compared among the pellets made, the durability of the D1FCr-L and D3FCr-L pellets had higher values than that of the D0FCr-L pellet (Figure 6). The results suggested that the stickiness property of biofilm-based FCR is more potent than that of starch-based NFCR. The values of bulk density, durability index, and pellet production yield samples were listed in Table 1. The maximum durability index of 99.56 ±0.1% and pellet production yield of 93.0±0.3% were also found when D3FCr was used.

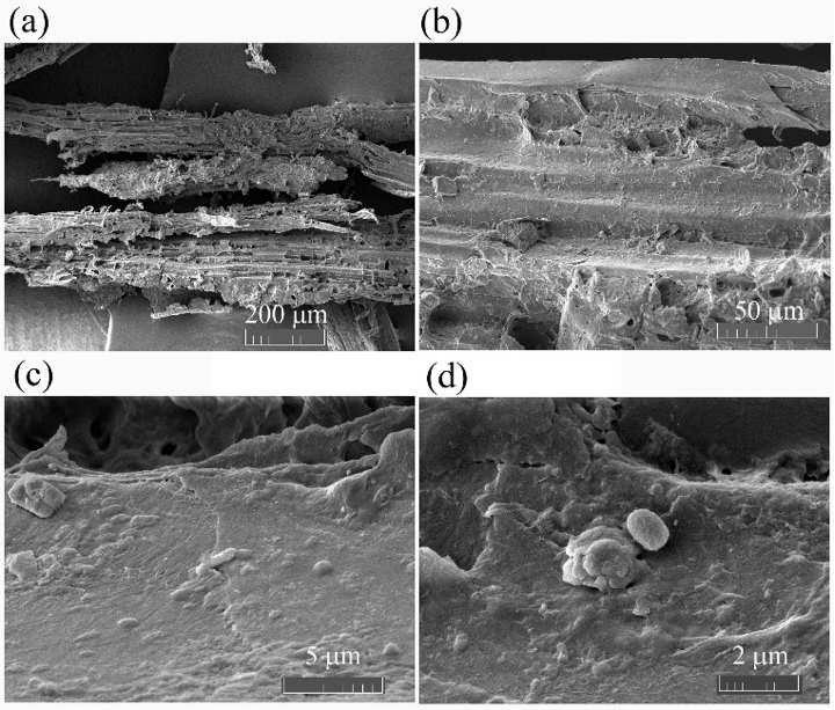

Fig. 4. SEM images of the D12FCr particles. (a) Decaying particles. (b) Porous structure on a piece of decaying wood. (c-d) Bacterial biofilms (the scales are as indicated).

According to the above-mentioned findings (Figure 3), biofilm was identified adhering to the surface of the FCR particles, as opposed to the starch granules found associated with the NFCR particles (Figure 2). The finding implies the starch granules was utilized for growth and biofilm production. For the starch-based NFCR, the binding property is likely due to the presence of starch granules revealed in this study (Figure 2), which aid in pelletizing, lubricating, and strengthening the pellet matrix at elevated temperatures. Previous research suggests that the mechanism of action is primarily based on gelatinized starch polymers formed with steam within the matrix during pelletizing, which may rely on the polarity of large amounts of OH groups (from glucose units and moisture) to form cohesive forces and connect the inter-particles with oppositely charged atoms, such as the accessible OH groups on the outer sugar moieties of cellulose and hemicellulose fibers [15], [19]-[20].

Extracellular polymeric substances (EPS) in biofilm matrices function in nature as hydrated bio-glue and biopolymers in nature, attaching producing microbes to solid surfaces [21]-[25]. Unlike starch, EPS polysaccharides (on FCR particles) contain not only the OH groups on sugars but also a variety of hydrophilic and negatively charged functional groups capable of generating far greater cohesive forces via ionic and hydrophilic interactions than the forces generated in starch molecules using mostly the dipole moments of the OH groups [22]–[25], [30]. A previous XRD study reported that Cr biomass contained a high proportion of calcium (ca. 20% of inorganic ashes) [36]. Some of the calcium element is likely to be divalent cations (Ca^{2+}), which may aid in the formation of ionic linkages with negatively charged functional groups [24], [30]. In a less potent way, the generation of binding forces can be aided by other EPS macromolecules, including polar, acidic, and basic amino acid side chains from proteins, negatively charged phosphodiester moieties from nucleotides, and fatty acids from lipids.

In Figures 5 to 7, the optimal fermentation time is 3 days, and longer fermentation results in a decrease in pellet quality. After day 3, rotting biomass fibers increased (Figure 4) and altered biofilm characteristics. As a result, the values of bulk density, durability index, and pellet production yield of D5FCr-L, D7FCr-L, and D12FCr-L decreased correspondingly (Figure 6). The results imply that prolonging fermentation for longer than 3 days reduces the adhesive property of the FCR. This is because microorganisms utilize biomass polymers as nutrients for growth and biofilm production. Consequently, available substrates decreased, microbes entered the stationary growth phase, and the number of rotting biomass fibers increased. A similar trend was seen when production yield was investigated (Figure 7).

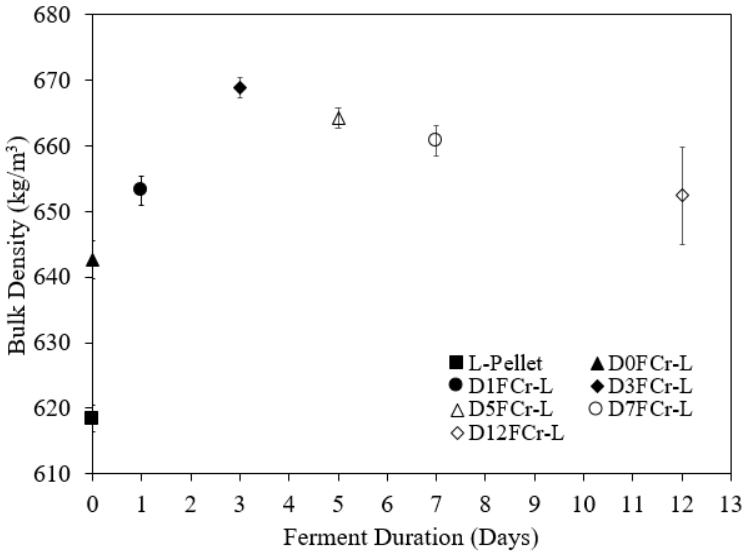

Fig. 5. Relationship between bulk density and ferment duration.

3.3 Effect of Fermented and Non-fermented Cr on HHV

HHVs of the Cr additive and pellet samples are listed in Table 2. The HHV of Cr was the lowest (17.01 ± 0.25 MJ/kg), while that of L-pellet was the highest (20.43 ± 0.32 MJ/kg). Since L-NFCR pellet and L-FCR pellet were produced from a mixture of Cr-based additives and L-wood, the HHV of these pellets should not be higher than that of L-pellet and not lower than that of Cr. HHV may be predicted by the following equation,

$$HHV_{mix,pellet} = y_{Cr} HHV_{Cr} + y_{L-wood} HHV_{L-wood} \quad (1)$$

where y_{Cr} and $y_{L\text{-}wood}$ represented the mass fraction of Cr and L-wood in L-NFCR pellet, respectively. The prediction result is shown in Figure 8. A mixing ratio of 100% was L-pellet, while 0% was Cr. A mixing ratio above 50% indicated that L-wood content was greater than Cr content. The prediction trend indicated a linear relationship between HHV and mixing ratio. The HHV of D0FCr-L, D1FCr-L, and D3FCr-L pellets agreed well with the predicted trend. The experimental HHV for D5FCr-L and D7FCr-L pellets was substantially lower

than the predicted trend. These findings indicated that converting starch to biofilm had no significant effect on Cr HHV. Equation 1 can thus be used to estimate the HHV of these pellets (D0FCr-L, D1FCr-L, and D3FCr-L). When the fermentation period was longer than 3 days, the release rate of fixed carbon in Cr (into the atmosphere as CO_2) increased. This explanation can be confirmed by the massive increase in rotting biomass fibers (Figure 4), which corresponds to the smaller HHV values of the D5FCr-L and D7FCr-L pellets.

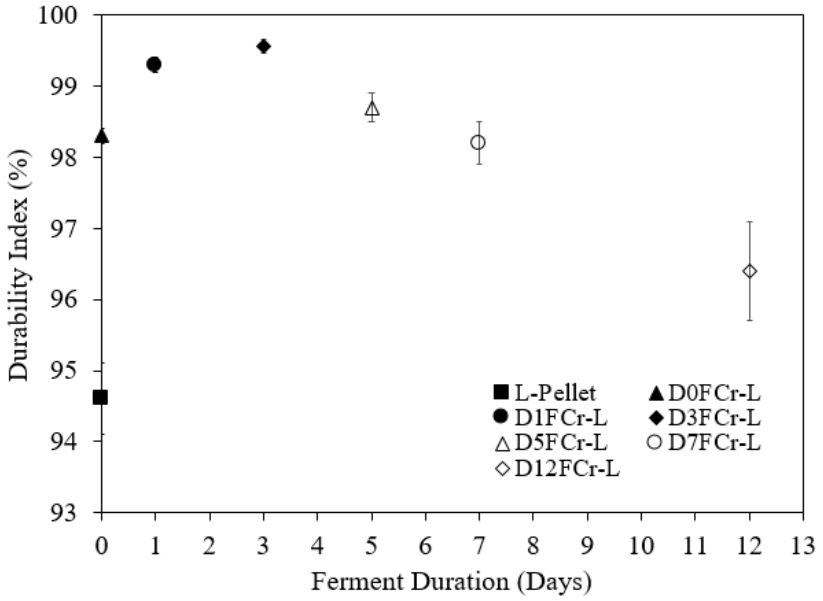

Fig. 6. Relationship between pellet durability index and ferment duration.

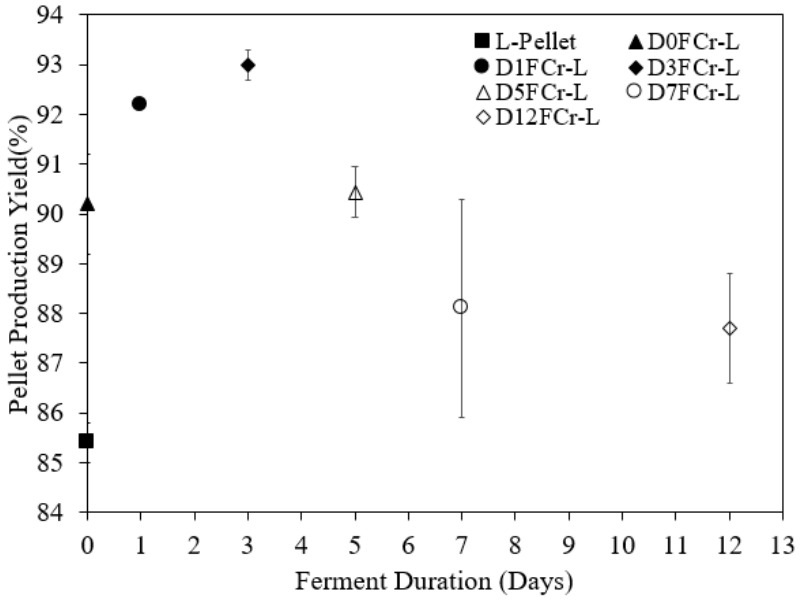

Fig. 7. Relationship between pellet production yield and ferment duration.

Table 1 Production yields and the physical characteristics of the pellet products.

Pellet sample	Yield, %	Bulk density, kg/m^3	Durability, %
L-pellet	85.4(±0.4)	618.4 (± 2.0)	94.6 (±0.5)
D0FCr-L	90.2(±1.0)	642.6 (±2.9)	98.3 (±0.1)
D1FCr-L	92.2(±0.1)	653.2 (±2.2)	99.3 (±0.1)
D3FCr-L	93.0(±0.3)	668.9 (±1.5)	99.5 (±0.1)
D5FCr-L	90.4(±0.5)	664.2 (±1.5)	98.7 (±0.2)
D7FCr-L	88.1(±2.2)	660.7 (±2.3)	98.2 (±0.3)
D12FCr-L	87.7(±1.1)	652.4 (±7.5)	96.4 (±0.7)

The number in parenthesis indicates standard deviation

Table 2 Higher heating values (HHVs) of the Cr additive and pellet samples.

Pellet sample	HV (MJ/kg)
Cr	17.01±0.25
L-pellet	20.43±0.32
D0FCr-L	19.42±0.21
D1FCr-L	19.39±0.16
D3FCr-L	19.50±0.26
D5FCr-L	19.22±0.23
D7FCr-L	18.79±0.18
D12FCr-L	n.d.[a]

[a] n.d., not determined.
The numbers in parenthesis indicate the standard deviations

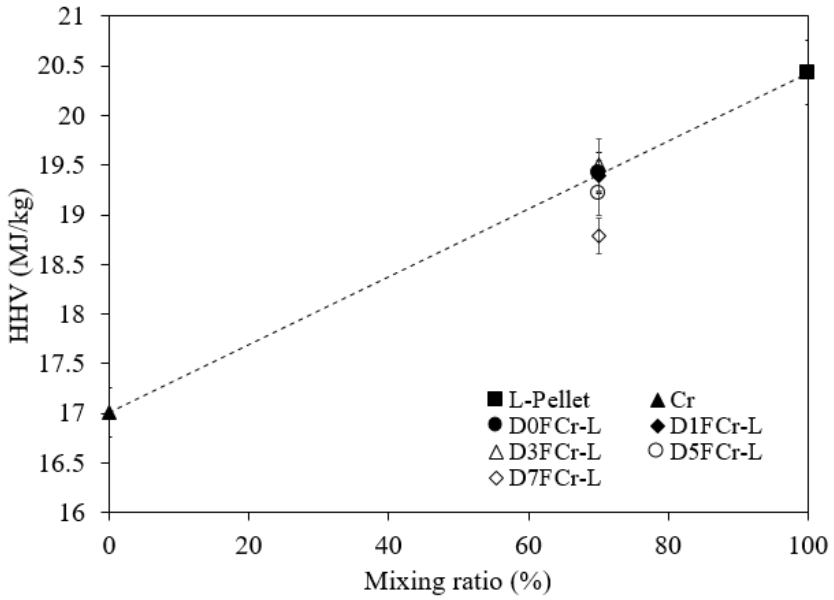

Fig. 8. Relationship between HHV and mixing ratio. This ratio displayed the percentage of L-wood content in produced pellet.

4. CONCLUSION

This study has successfully enhanced the adhesive quality of a starch-based Cr, an agricultural residue, using an energy-saving microbiological procedure. The microbial biofilm had a higher adhesive quality than the starch in non-fermented Cr. The conversion of starch to biofilm had no significant effect on Cr HHV. Day 3 of incubation was shown to be the optimal fermentation time. After day 3, rotting biomass fibers increased and altered the biofilm, resulting in a decrease in adhesive quality and HHV. Finally, a novel fermented Cr derived from biofilm is proposed as an improved biomass-binding additive for the production of durable, high-quality biomass pellets. The findings of this study will help with the exploitation and management of starch-rich agricultural wastes, particularly cassava harvesting residuals.

ACKNOWLEDGEMENT

The Silpakorn University Research, Innovation, and Creative Fund, as well as the Department of Mechanical Engineering, Faculty of Engineering and Industrial Technology, Silpakorn University, Thailand, are funding this study. The authors would like to thank the Laboratory of Innovation Fuels and Energy at Silpakorn University's Department of Mechanical Engineering, Faculty of Engineering and Industrial Technology

REFERENCES

[1] Huang Y.F., Cheng P.H., Chiueh P.T., and Lo S.L.L., 2017. Leucaena biochar produced by microwave torrefaction: Fuel properties and energy efficiency. *Applied Energy* 204(15): 1018 – 1025.

[2] Anish M., Arunkumar T., Jayaprabakar J., Nivin Joy T., Obaid S.A., Alfarraj S., Raj M.M., and Markos M., 2022. Analysis of variable compression ratio engine using biodiesel when incorporated with metal oxides from chemical and biological resources. *Journal of Nanomaterials*. Article ID 9221720.

[3] Hoogwijk M., Faaij A., Eickhout B., Vries B., and Turkenburg W., 2005. Potential of biomass energy out to 2100, for four IPCC SRES land-use scenarios. *Biomass Bioenergy* 29: 225 – 257.

[4] Yokoyama S., Ogi T. and Nalampoon A., 2000. Biomass energy potential in Thailand. *Biomass Bioenergy* 18(5): 405-410.

[5] The Food and Agricultural Organization of the United Nation, FAOSTAT on Cassava Production/Crops Primary/Thailand/Years 2018-2020.

[6] Stelte W., Holm J.K., Sanadi A.R., Barsberg S., Ahrenfeldt J., and Henriksen U.B., 2011. A study of bonding and failure mechanisms in fuel pellets from different biomass resources. *Biomass and Bioenergy* 35(2): 910 – 918.

[7] García-Maraver A., Popov V., and Zamorano M., 2012. A review of European standards for pellet quality. *Renewable Energy* 36(12): 3537 – 3540.

[8] Joy N., Mariadhas A., Jayaraman J., Venugopal J., Susmi S., and Pensigamani B., 2022. The effects of nanoparticles as a biodiesel ingredient on the performance of a VCR diesel engine. *Transactions of the Canadian Society for Mechanical Engineering*. 47: 202 – 210.

[9] Temmerman M., Rabier F., Jensen P.D., Hartmann H., and Bohm T., 2006. Comparative study of durability test methods for pellets and briquettes. *Biomass and Bioenergy* 30(11): 964 – 972.

[10] Thapa S.. and Engelken R., 2020. Optimization of pelleting parameters for producing composite pellets using agricultural and agro-processing wastes by Taguchi-Grey relational analysis. *Carbon Resources Conversion* 3: 104 – 111.

[11] Bency P., Anish M., Jayaprakash V., Jayaprabakar J., Yanmaz E., Joy N., and Ramulu P.J., 2023. Comparative Assessment of Compression Strength of Solid Biobriquette using Different Binding Materials. *Journal of Nanomaterials*. Aricle ID 3685782.

[12] Rajput S.P., Jadhav S.V., and Thorat B.N., 2020. Methods to improve properties of fuel pellets obtained from different biomass sources: Effect of biomass blends and binders. *Fuel Processing Technology* 199: 106255.

[13] Anish M., Bency P., Jayaprabakar J., Joy N., Jayaprakash V., Sahaya Susmi S.K., Kumar J.A., Ansar S., and Rezania S., 2022. An evaluation of biosynthesized nanoparticles in biodiesel as an enhancement of a VCR diesel engine. *Fuel* 328(6): 125299.

[14] Lee J.S., Sokhansanj S., Lau A.K., Lim J., and Bi X.T., 2021. Moisture adsorption rate and durability of commercial softwood pellets in a humid environment. *Biosystems Engineering* 203: 1 – 8.

[15] Antonio T., 2019. A review on biomass: importance, chemistry, classification, and conversion. *Biofuel Research Journal* 6(2): 962 – 979.

[16] Bootten T.J., Harris P.J., Melton L.D., and Newman R.H., 2004. Solid-state 13C-NMR spectroscopy shows that the xyloglucans in the primary cell walls of mung bean (*Vigna radiata* L.) occur in different domains: a new model for xyloglucan-cellulose interactions in the cell wall. *Journal of Experimental Botany* 55(397): 571 – 583.

[17] Anukam A., Berghel J., Henrikson G., Frodeson S., and Ståhl M., 2021. A review of the mechanism of bonding in densified biomass pellets. *Renewable and Sustainable Energy Reviews* 148: 111249.

[18] Westbye P., Köhnke T., Glasser W., and Gatenholm P., 2007. The influence of lignin on the self-assembly behaviour of xylan rich fractions from birch (*Betula pendula*). *Cellulose* 14(6): 603 – 613.

[19] Anukam A., Berghel J., Frodeson S., Famewo E.B., and Nyamukamba P., 2019. Characterization of pure and blended pellets made from Norway spruce and pea tarch: a comparative study of bonding mechanism relevant to quality. *Energies* 12(23): 4415 – 4436.

[20] Anukam A., Berghel J., Famewo E.B., and Frodeson S., 2020. Improving the understanding of the bonding mechanism of primary components of biomass pellets through the use of advanced analytical instruments. *Journal of Wood Chemistry and Technology* 40: 15–32.

[21] Li Z., Ren L., Qiao Y., Li X., Zheng J., Ma J., and Wang Z., 2022. Recent advances in membrane biofilm reactor for micropollutants removal: Fundamentals, performance and microbial communities. *Bioresource Technology* 343: 126139 – 126153.

[22] Ghosh P.K. and T.K. Maiti. 2016. Structure of extracellular polysaccharides (EPS) produced by rhizobia and their functions in legume-bacteria symbiosis: - A review. *Achievements in the Life Sciences* 10(2): 136 – 143.

[23] Götz F., 2002. *Staphylococcus* and biofilms. *Molecular Microbiology* 43(6): 1367 – 1378.

[24] Boyd A. and A.M. Chakrabarty. 1995. Pseudomonas aeruginosa biofilms: role of the alginate exopolysaccharide. *Journal of Industrial Microbiology* 15: 162 – 168.

[25] Al-Fattani M.A. and L.J. Douglas, 2006. Biofilm matrix of *Candida albicans* and *Candida tropicalis*: chemical composition and role in drug resistance. *Journal of Medical Microbology* 55(8): 999 – 1008.

[26] Relucenti M., Familiari G., Donfrancesco O., Taurino M., Li X., Chen R., Artini M., Papa R., and Selan L., 2021. Microscopy methods for biofilm imaging: focus on SEM and VP-SEM pros and cons. *Biology (Basel)* 10(1): 51 – 67.

[27] Kaplan J.B., Ragunath C., Velliyagounder K., Fine D.H. and Ramasubbu N., 2004. Enzymatic detachment of *Staphylococcus epidermidis* biofilms. *Antimicrobial Agents and Chemotherapy* 48(7): 2633 – 2636.

[28] Nivens D.E., Ohman D.E., Williams J., and Franklin M.J., 2001. Role of alginate and its O acetylation in formation of *Pseudomonas aeruginosa* microcolonies and biofilms. *Journal of Bacteriology* 183: 1047 – 1057.

[29] Freitas F., Alves V.D., Carvalheira M., Costa N., Oliveira R., and Reis M.A.M, 2009. Emulsifying

behaviour and rheological properties of the extracellular polysaccharide produced by *Pseudomonas oleovorans* grown on glycerol byproduct. *Carbohydrate Polymers* 78(3): 549 – 556.

[30] Giavasis I., Harvey L.M., and McNeil B., 2000. Gellan gum. *Critical Reviews in Biotechnology* 20(3): 177 – 211.

[31] Rinaudo M., 2014. Biomaterials based on a natural polysaccharide: alginate. *TIP* 17(1): 92 – 96.

[32] Birch J., Van Calsteren M.R., Pérez S., and Svensson B., 2019. The exopolysaccharide properties and structures database: EPS-DB. Application to bacterial exopolysaccharides. *Carbohydrate Polymers* 205(1): 565 – 570.

[33] Akbar A., Aslam U., Asghar A. and Aslam Z., 2021. Effect of binding materials on physical and fuel characteristics of bagasse-based pellets. *Biomass and Bioenergy* 150: 106118.

[34] Wang Z., Zhai Y., Wang T., Wang B., Peng C., and Li C., 2020. Pelletizing of hydrochar biofuels with organic binders. *Fuel* 280: 118659.

[35] Kaliyan N. and R.V. Morey. 2009. Factors affecting strength and durability of densified biomass products. *Biomass and Bioenergy* 33(3): 337 – 359.

[36] Kanoksilapatham W., Ogawa M., and Intagun W., 2020. Effects of clay and temperature on the slag formation of two biomass fuels: Wood from *Acacia mangium* and rhizome residual from *Manihot esculenta*. *Renewable Energy* 156: 213 – 219.

[37] Ndubuisi N.D. and A.C.U. Chidiebere 2018. Cyanide in cassava: A review. *International Journal of Genomics and Data Mining*. 02: 118. DOI: 10.29011/2577-0616.000118

[38] Coulin P., Farah Z., Assanvo J., Spillmann H., and Puhan Z., 2006. Characterisation of the microflora of attiéké, a fermented cassava product, during traditional small-scale preparation. *International Journal of Food Microbiology* 106(2):131-136.

[39] ASTM International. ASTM E 873-82, Standard test method for bulk density of densified particulate biomass fuels; 2006.

[40] ASTM International. ASTM E 711-87, Standard test method for gross calorific value of refuse-derived fuel by the bomb calorimeter; 2004.